Intensity of the Polarized Raman Band at 1340−1345 cm^{-1} As an Indicator of Protein α-Helix Orientation: Application to Pf1 Filamentous Virus†

Masamichi Tsuboi,‡ Mika Suzuki,‡ Stacy A. Overman,§ and George J. Thomas, Jr.*,§

Department of Fundamental Science, Iwaki-Meisei University, Iwaki, Fukushima 970, Japan, and Division of Cell Biology and Biophysics, School of Biological Sciences, University of Missouri−Kansas City, Kansas City, Missouri 64110

Received August 12, 1999; Revised Manuscript Received November 18, 1999

ABSTRACT: Raman spectra of oriented α-helical protein molecules exhibit a prominent band near 1340−1345 cm^{-1}, the intensity of which is highly sensitive to molecular orientation. Polarization of the 1340−1345 cm^{-1} marker is evident in Raman spectra of α-helical poly-L-alanine (αPLA) and α-helical poly-γ-benzyl-L-glutamate (αPBLG). Corresponding polarization is also observed in Raman spectra of the filamentous virus Pf1, which is an assembly of α-helical coat protein molecules. In αPLA and αPBLG, we assign the band to a normal mode of symmetry type E_2 and specifically to a vibration localized in the (O═C)−C$^{\alpha}$−H linkages of the main chain peptide group. Although strict helical symmetry does not apply to coat subunits of filamentous viruses, an approximate E_2-type mode may be presumed to account for a corresponding Raman band of Pf1 and fd filamentous viruses. Spectroscopic studies of *N*-methylacetamide and isotopically-edited fd viruses support the present assignment of the 1340−1345 cm^{-1} band. Polarization anisotropy indicates that this band may be exploited as a novel indicator of protein α-helix orientation. Application of this approach to the polarized Raman spectrum of Pf1 suggests that, on average, the axis of the α-helical coat protein subunit in the native virion structure forms an angle of 20 ± 10° with respect to the virion axis.

Vibrational spectroscopy is a sensitive probe of local structure in biological macromolecules and their assemblies (*1*−*4*). The structural information obtainable from vibrational spectra can be enhanced by investigating oriented biomolecules using polarized radiation (*5*−*7*). Recent applications have provided new insights into the orientations of secondary structure domains and specific side chains in many different types of protein assemblies (*8*−*12*). These applications make use of well-characterized amide modes of the peptide main chain and various ring modes of aromatic side chains. Further development of polarized vibrational spectroscopy requires improved assignments for the numerous other bands that exhibit polarization effects in infrared and Raman spectra.

Of particular interest are vibrational modes related to the polypeptide backbone, which when properly investigated by either polarized Fourier-transform infrared (FTIR)[1] or polarized Raman methods, can yield the directionality of protein secondary structure elements. Much attention has been given to interpreting peptide and protein vibrational bands of the spectral interval 1300−1400 cm^{-1} of FTIR and Raman spectra, including those obtained by the related techniques of vibrational circular dichroism (VCD), Raman optical activity (ROA), and ultraviolet−resonance Raman (UVRR) spectroscopy (*13*−*17*). The focus of the present work is on the prominent band observed near 1340−1345 cm^{-1} in Raman spectra of polypeptides and proteins that contain α-helical secondary structure. This Raman band is particularly intense in spectra of α-helical poly-L-alanine (αPLA) (*18*) and filamentous viruses (*19*−*21*) and exhibits an apparent counterpart in FTIR (*22*), ROA (*17*), VCD (*13*) and UVRR (*15*) spectra.

Vibrational modes specific to the α-helix have been extensively studied in αPLA (*18*, *22*, *23*) and αPBLG (*24*, *25*). Biological protein assemblies consisting exclusively or predominantly of α-helical subunits, such as the filamentous viruses Pf1 and fd, also serve as effective models for the α-helix (*16*, *19*, *20*, *26*). Relatively well understood are the amide I and amide III modes of the α-helix, which occur in the intervals 1645−1654 and 1270−1310 cm^{-1}, respectively, of the Raman spectrum and 1650−1655 and 1275−1306 cm^{-1}, respectively, of the FTIR spectrum. The amide II mode of the α-helix is prominent only in infrared spectra (1515−1555 cm^{-1}), although pre-resonance-enhanced amide II Raman intensity can be observed near 1555 cm^{-1} when UV excitation is employed.

The Raman band observed near 1340−1345 cm^{-1} in spectra of model α-helices has the potential to serve as a general marker of α-helix structure. Confirmation of this assignment would provide a new α-helix marker for diagnosis of protein secondary structure in nucleoprotein assemblies, for which the conventional amide I and amide III regions may be overlapped by bands due to nucleic acid components. The work presented here has also been moti-

† Paper LXVIII in the series Structural Studies of Viruses by Raman Spectroscopy. Supported by NIH Grant GM50776.

* To whom correspondence should be addressed. Phone: 816-235-5247. Fax: 816-235-1503. E-mail: <thomasgj@umkc.edu.

‡ Iwaki-Meisei University.

§ University of Missouri−Kansas City.

[1] Abbreviations: FTIR, Fourier-transform infrared; NMA, *N*-methylacetamide; αPLA, α-helical poly-L-alanine; αPBLG, α-helical poly-γ-benzyl-L-glutamate; VCD, vibrational circular dichroism; ROA, Raman optical activity.

10.1021/bi9918846 CCC: $19.00
Published on Web 02/12/2000

vated by the recent observation that deuteration of $C^{\alpha}H$ groups in the α-helical coat protein subunits of fd leads to a significant loss of Raman intensity near 1345 cm^{-1}, attributable to the deuteration shift of a complex mode involving both C^{α}—H bending and C—C^{α} stretching internal coordinates (*20, 21*). The present analysis supports assignment to the (O═C)—C^{α}—H network and suggests a role for the 1340−1345 cm^{-1} Raman band as an indicator of α-helix orientation in protein assemblies.

EXPERIMENTAL METHODS

1. Materials. Poly-γ-benzyl-L-glutamate (PBLG; degree of polymerization 1140), poly-L-alanine (PLA; molecular weight range 1000−5000), and standard reagents were purchased from Sigma Chemical Co. (St. Louis). Unidirectional orientation of PBLG and PLA films or fibers was achieved by mechanical stroking of viscous dioxane solutions during evaporation.

2. Preparation of Virus. Wild-type Pf1 virus was obtained from Dr. Loren A. Day, Public Health Research Institute, New York, and grown on *Pseudomonas aeruginosa* strain K. Growth media and standard reagents were obtained from Sigma and Fisher Scientific (St. Louis, MO).

Pf1 virus was grown in MS medium containing 1% glucose and 4 mM $CaCl_2$. Mature viral particles, extruded through the bacterial cell membrane and into the growth medium, were collected by precipitation with poly(ethylene glycol) (2%) and NaCl (0.5 M) followed by low-speed centrifugation. The virus precipitate was resuspended in 10 mM Tris (pH 7.8 ± 0.2), and the resulting suspension was purified by four cycles of pelleting at 330000 *g* for 1.5 h and resuspension of the pellet in 10 mM Tris buffer. This procedure accomplishes essentially complete removal of excess NaCl and produces the low-salt form of the virus. [Effects of salt concentration on Raman spectra of filamentous viruses have been reported elsewhere (*19*).] Typically, 20−30 mg of purified virus was obtained from a 1-L preparation. Pf1 concentration was determined by UV spectrophotometry using an extinction coefficient at 270 nm of 2.06 $mL \cdot mg^{-1} \cdot cm^{-1}$ (*27*).

3. Instrumentation. Polarized vibrational spectra of oriented Pf1 virus and polypeptides were obtained using infrared (Micro-FTIR-100) and Raman (Micro-Raman NRS-2000) microscopes manufactured by Jasco (Tokyo, Japan). Polarized Raman spectra were excited at 514.5 nm. Unpolarized Raman spectra were obtained on a Nicolet FT-Raman 950 spectrometer using 1063 nm excitation. Raman spectra of fd virus were obtained on a Spex Model 500M spectrometer (ISA, Edison, NJ) using 514.5 nm excitation, as described previously (*20, 21*).

RESULTS AND DISCUSSION

1. The Raman Band of fd Virus near 1340−1345 cm^{-1} Is Due to a Vibration Localized in the (O═C)—C^{α}—H Moiety of the α-Helical Coat Protein Subunit

The Raman spectrum of fd virus exhibits a very strong and complex band within the interval 1340−1345 cm^{-1}, which has been assigned unambiguously to the viral coat protein subunit (*19*). Among the many normal modes contributing to the band envelope are an indole ring vibration of the Trp-26 side chain (*28, 29*) and CH deformation

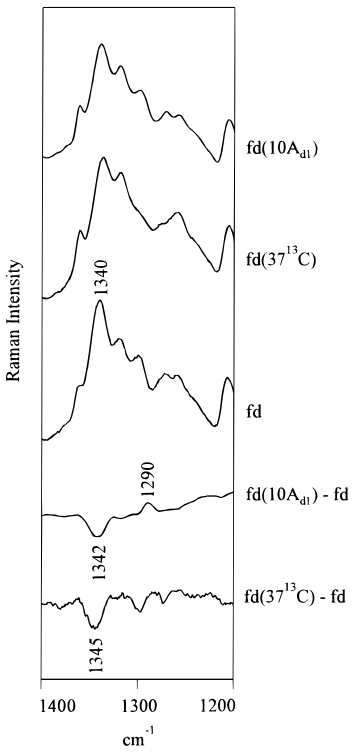

FIGURE 1: Raman spectra (1400−1200 cm^{-1}, 514.5 nm excitation) of isotopomers of fd virus (each at 80 mg/mL in 10 mM Tris, pH 7.8): fd($10A_{d1}$) incorporates ^{2}H at C^{α} of each of 10 Ala residues of the coat subunit; fd($37^{13}C$) incorporates ^{13}C at 37 C═O sites; fd is unlabeled. The normalized difference spectra (lower two traces) computed with isotopically labeled virus as minuend and unlabeled virus as subtrahend demonstrate the diminished Raman intensity near 1340−1345 cm^{-1} with isotope substitutions. For consistency with subsequent figures showing infrared spectra, the cm^{-1} units of the abscissa are shown decreasing from left to right. Further details are given in refs *20* and *21*.

vibrations of various aliphatic side chains (*21*). Surprisingly, the intensity of the 1340−1345 cm^{-1} band envelope is diminished significantly by ^{13}C substitution of peptide carbonyl sites and deuterium substitution of main chain C^{α} sites (*20, 21*). This indicates that the band intensity is derived in substantial part from a vibrational mode localized in the main chain (O═C)—C^{α}—H network. Both the (O═C)—C^{α}—D and (O═^{13}C)—C^{α}—H isotopomers exhibit significantly lower intensity than the unlabeled virus at 1345 cm^{-1} (*20, 21*), indicating that the peptide (O═C)—C^{α}—H repeat is characterized by a Raman-active normal mode near 1345 cm^{-1}. This spectral contribution, depicted in Figure 1, has been ascribed to a vibration involving the C^{α}—H bend and C—C^{α} stretch internal coordinates of the α-helical coat protein subunit of the native virus (*20*).

Studies of additional fd isotopomers have demonstrated that the amide III mode of the coat protein α-helix is not a significant contributor to the 1340−1345 cm^{-1} band envelope in fd (*20*). The fact that the fd band near 1340−1345 cm^{-1} comprises a contribution from the C^{α}−H bend and C−C^{α} stretch internal coordinates, but not from the amide III mode, is corroborated by several additional lines of evidence, as discussed next.

(a) The Protein Amide III Mode Is Not Expected as High as 1340−1345 cm^{-1}. Liquid *N*-methylacetamide (NMA), which contains intermolecular NH···O═C hydrogen bonds simulating those of a protein, exhibits a prominent vibrational

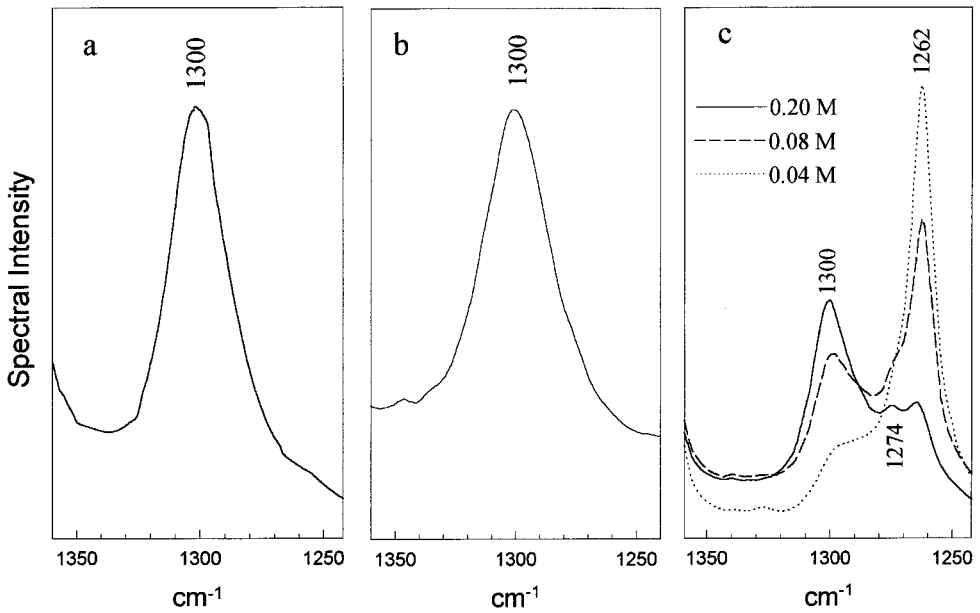

FIGURE 2: Vibrational spectra of *N*-methylacetamide in the 1350−1250 cm^{-1} region: (a) infrared spectrum of pure liquid *N*-methylacetamide; (b) Raman spectrum (1063 nm excitation) of pure liquid *N*-methylacetamide; (c) infrared spectra of 0.20 (—), 0.08 (- - -), and 0.04 (···) M solutions of *N*-methylacetamide in CCl_4, obtained with CaF_2 liquid-cell windows and optical paths of 0.20, 0.50, and 1.0 mm, respectively.

band at 1300 cm^{-1} (*30*). In the absence of hydrogen bonding (CCl_4 solution), this band falls to 1262 cm^{-1} (Figure 2). Normal coordinate calculations show that the NMA band in the 1262−1300 cm^{-1} interval is due to an amide III-like vibration, i.e., involving primarily C−N stretching with some contribution from N−H in-plane bending (*30*). Accordingly, it is unlikely that an α-helical protein would exhibit an amide III vibrational band with a wavenumber value as high as 1340−1345 cm^{-1}. This conclusion is also supported by a recent theoretical analysis (*31*).

(b) A C^{α}—H Bending Mode of L*-Alanyl-*L*-alanine Occurs near 1330 cm^{-1}.* The IR spectrum of isobutane [$CH(CH_3)_3$] exhibits a doubly degenerate C—H bending vibration at 1328 cm^{-1} (*32*). In the case of L-alanine the degeneracy is eliminated, which results in two C—H bend components at 1358 and 1306 cm^{-1} (*33*, *34*). L-Alanyl-d_1-L-alanine in D_2O solution contains no NH group and a single $C^{\alpha}H$ group and, accordingly, is expected to give nearly pure C^{α}—H bending modes. Diem et al. (*13*) report these at 1330 and 1279 cm^{-1} in the infrared. Normal coordinate analysis suggests that for the 1330 cm^{-1} vibration the hydrogen atom displacement takes place in the C—C^{α}—H plane, whereas for the 1279 cm^{-1} vibration the displacement is perpendicular to the plane (*13*). On the basis of these findings, it can be inferred that the 1345 cm^{-1} band of the (O═C)—C^{α}—H network of the α-helical coat protein of fd corresponds more closely to the 1330 cm^{-1} band of L-alanyl-d_1-L-alanine than to an amide III-related mode.

(c) Theoretical Analysis of the ^{13}C Isotope Effect in fd Shows That the 1340−1345 cm^{-1} Band Is Not Due to a Pure C^{α}−H Bending Mode. The method developed by Nakagawa and Mizushima (*35*) for tetrahedral $HCXY_2$ molecules can be applied to the data obtained on unlabeled and ^{13}C-labeled fd isotopomers to assess whether the observed ^{13}C isotope effect is consistent with a pure C^{α}−H bending vibration. For this purpose, we adopt the pair of local symmetry coordinates, $S_1 \equiv 2R_{23} - R_{21} - R_{19}$ and $S_2 \equiv R_{21} - R_{19}$, where R_{23}, R_{21}, and R_{19} are the valence angles shown in Figure 3.

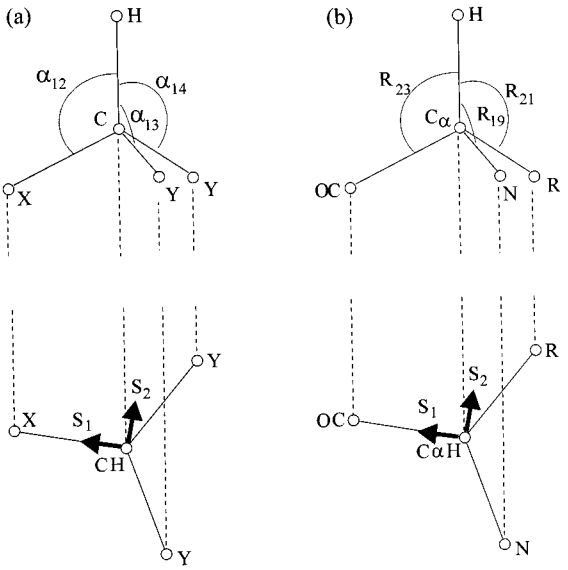

FIGURE 3: (a) Tetrahedral $HCXY_2$ molecule with a plane of symmetry containing H−C−X. (b) Amino acid residue of a polypeptide chain. Top views are perpendicular to the C−H (or C^{α}−H) bond, and lower views are along the bond. Symmetry coordinates S_1 and S_2 are shown. (S_1 is considered to correspond to the C^{α}−H bending coordinate in the 1345 cm^{-1} normal mode of the fd coat protein.)

Note that the present choice of S_1 and S_2 (Figure 3) differs from the symmetry coordinates, $H_{\alpha}b1 \equiv 2R_{21} - R_{19} - R_{23}$ and $H_{\alpha}b2 \equiv R_{19} - R_{23}$, chosen by Lee and Krimm in a similar treatment of αPLA (*23*). We favor the present choice because the bending force constants for R_{21} (C^{β}−C^{α}−H valence angle bend) and R_{19} (N−C^{α}−H valence angle bend) should be fairly close to one another and much smaller than the bending force constant for R_{23} (C−C^{α}−H valence angle bend), as appropriate for the tetrahedral $HCXY_2$ model. Therefore, the force constant for S_1 must be greater than that for S_2, in accord with the experimental data on L-alanyl-d_1-L-alanine, indicating frequencies of 1330 and 1279 cm^{-1}, respectively (*13*).

Symmetry coordinates for the CH bending vibrations of symmetry species A′ and A″ of the $HCXY_2$ system can be given in terms of the valence angles α_{ij} of Figure 3a as follows:

$$A': \quad S_1 = \Delta(2\alpha_{12} - \alpha_{13} - \alpha_{14})/6^{1/2} \tag{1}$$

$$A'': \quad S_2 = \Delta(\alpha_{13} - \alpha_{14})/2^{1/2} \tag{2}$$

The corresponding diagonal elements of the inverse kinetic energy matrix (G) are

$$G(S_1,S_1) = [(3/2)\mu_H + (3/2)\mu_C]\rho_H^2 + (2/3)\mu_X\rho_X^2 + (1/3)\mu_Y\rho_Y^2 + \mu_C[(2/3)\rho_H\rho_X + (1/3)\rho_H\rho_Y + (2/3)\rho_X^2 - (10/9)\rho_X\rho_Y + (11/18)\rho_Y^2] \tag{3}$$

$$G(S_2,S_2) = [(3/2)\mu_H + (3/2)\mu_C]\rho_H^2 + \mu_Y\rho_Y^2 + \mu_C[(1/6)\rho_Y^2 + \rho_H\rho_Y] \tag{4}$$

Here, μ_H, μ_C, μ_X, and μ_Y are reciprocals of the H, C, X, and Y atomic masses, respectively, and ρ_H, ρ_X, and ρ_Y are reciprocals of the C—H, C—X, and C—Y bond lengths, respectively. Note that $G(S_1,S_1)$ depends upon μ_X and therefore differs for ^{12}C and ^{13}C isotopomers. With $\mu_H = 1$, $\mu_C = \mu_X = \mu_Y = 1/12$, $\rho_H = 1/1.1$ A^{-1}, and $\rho_X = \rho_Y = 1/1.5$ A^{-1} for the unlabeled isotopomer, and with $\mu_X = 1/13$ for the ^{13}C═O isotopomer, eq 3 yields the ratio $G(S_1,S_1)/G^*(S_1,S_1) = 1.001\,324$, where the asterisk refers to the ^{13}C═O isotopomer. The corresponding frequency difference is calculated to be only -1 cm^{-1} (i.e., 1344−1345 cm^{-1}). Thus, no significant ^{13}C isotope effect is predicted for a "pure" CH bending mode. Accordingly, the normal vibration giving rise to the 1345 cm^{-1} band of fd is not likely to be such a localized C^α—H bending vibration and must involve at least one other internal coordinate, such as the C—C^α stretch of the (O═C)—C^α—H network.

Normal vibrations involving displacement of H in the $HCXY_2$ system require compensating displacements of atoms X (^{13}C) and/or Y (N and R) to fix the center of gravity. The prominent ^{13}C effect observed for the 1345 cm^{-1} vibration suggests, therefore, that displacement of H takes place in the (O═C)—C^α—H plane (Figure 3b), rather than in the direction perpendicular to this plane. Although it is clear that the 1345 cm^{-1} vibration of the fd coat protein α-helix is not a pure C^α—H bending mode, it is a mode that is localized in the (O═C)—C^α—H moiety of the peptide main chain and, on the basis of the observed C^α—D isotope shift (*21*), must contain a significant contribution from the C^α—H bend internal coordinate.

2. Vibrational Modes of the (O═C)—C^α—H Moiety in α-Helical Polypeptides

(a) Polarized Vibrational Spectroscopy of Poly-γ-benzyl-L-glutamate. Highly polymerized poly-γ-benzyl-L-glutamate forms an α-helical structure (αPBLG) that is readily drawn into well-oriented films or fibers suitable for investigation by polarized IR (*24*) and Raman (*25*) methods. To confirm key details of the previously reported polarized spectra, we have reexamined αPBLG as shown in Figure 4 (1250−1400 cm^{-1} region).

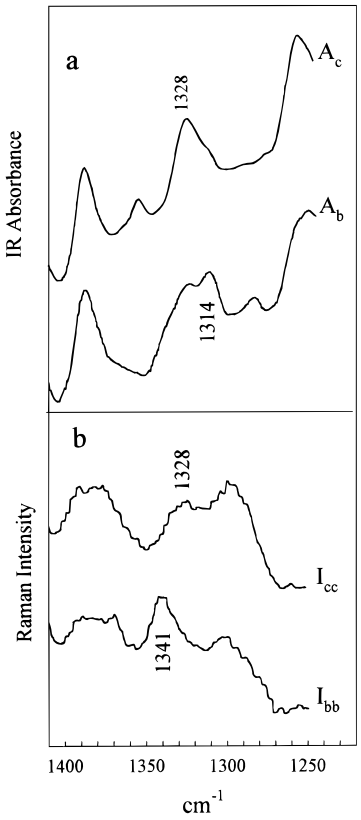

FIGURE 4: (a) Polarized infrared absorption spectra of an oriented film of PBLG with the electric vector of the absorbed radiation parallel (A_c, upper trace) and perpendicular (A_b, lower trace) to the fiber axis, *c*. (b) Polarized Raman spectra of an oriented fiber of PBLG with electric vectors of both the exciting and scattered beams either parallel to *c* (I_{cc}, upper trace) or perpendicular to *c* (I_{bb}, lower trace). Unidirectional orientation of the film or fiber was achieved by mechanical stroking of a viscous dioxane solution during evaporation.

In general, optically-active normal vibrations of the α-helix are classified into three symmetry types, A, E_1, and E_2, for which the phase differences between motions of adjacent peptide units are 0°, 100°, and 200°, respectively (*36*). With respect to IR spectra, vibrations of the A type are characterized by a transition moment direction along the helix axis (*c*), whereas for E_1 vibrations the transition moment direction is perpendicular to *c*, i.e., along *a* or *b*. E_2 vibrations are IR-inactive. For Raman spectra, A-type vibrations have nonzero principal-axis components (*aa*, *bb*, *cc*) of the Raman scattering tensor, whereas E_1 vibrations have nonzero *bc* and/or *ac* tensor components and E_2 vibrations have nonzero *ab* tensor components. By analyzing the spectra of Figure 4 and recalling that the I_{bb} spectrum contains the *ab*, *ba*, and *bb* tensor components, we deduce that the (O═C)—C^α—H mode of αPBLG has A, E_1, and E_2 components at 1328, 1314, and 1341 cm^{-1}, respectively. In the Miyazawa perturbation treatment (*37*), these frequencies should fit eqs 5−7, which

$$A: \quad \nu_0 + D_1 + D_3 = 1328 \tag{5}$$

$$E_1: \quad \nu_0 + D_1\cos 100 + D_3\cos 300 = 1314 \tag{6}$$

$$E_2: \quad \nu_0 + D_1\cos 200 + D_3\cos 600 = 1341 \tag{7}$$

requires that $\nu_0 = 1347$ cm^{-1}, $D_1 = 35$ cm^{-1}, and $D_3 = -54$ cm^{-1}. Here, ν_0 represents the unperturbed vibration of

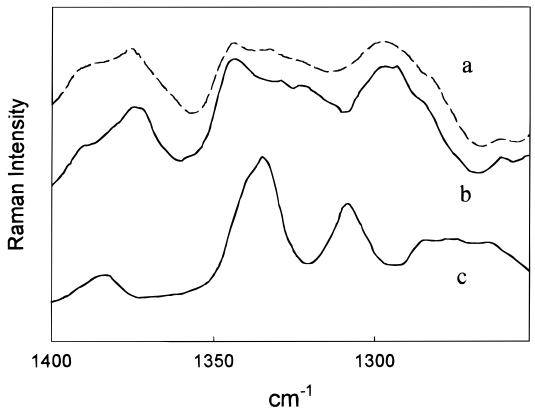

FIGURE 5: (a) Simulated unpolarized Raman spectrum of αPBLG ($I_{cc} + 2I_{bb}$), calculated from the data of Figure 4. (b) Experimental unpolarized Raman spectrum of αPBLG powder. (c) Experimental unpolarized Raman spectrum of αPLA.

the (O═C)—C^{α}—H group of αPBLG, which corresponds to a peptide that is hydrogen bonded nonspecifically (random coil), and D_1 and D_3 are the coupling parameters between neighboring and third next-neighboring peptides of the α-helix. It should be kept in mind that the significance of the parameters ν_0, D_1, and D_3 is dependent upon the basic assumption of the Miyazawa theory that the normal mode in question represents a localized vibration.

(b) Polarized Vibrational Spectroscopy of Poly-L-alanine. Polarized Raman studies of oriented αPLA fibers indicate an A mode at 1331 cm^{-1} and E_2 mode at 1337 cm^{-1} for the (O═C)—C^{α}—H vibration (*18*, *22*). Therefore, the ν_0, D_1, and D_3 values for αPLA do not differ greatly from those determined for αPBLG in eqs 5−7. However, N-deuteration effects observed for αPLA (1331 → 1327 and 1337 → 1324 cm^{-1}) (*18*) suggest very weak vibrational coupling between (O═C)—C^{α}—H and N—H bending modes.

(c) Unpolarized Raman Spectra of α-Helical Polypeptides. Figure 5 shows unpolarized Raman spectra in the region 1250−1400 cm^{-1} of randomly oriented (powder) samples of αPBLG and αPLA. [The Raman spectrum of randomly oriented αPBLG can also be simulated by appropriate addition of polarized spectra ($2bb + cc$), as shown in Figure 5 (top).] For both αPBLG and αPLA, the most intense Raman band occurs at 1340 cm^{-1}, which is close to the wavenumber value (1345 cm^{-1}) of the difference band observed in isotopic difference spectra of fd (*20*, *21*). In both αPLA and αPBLG the 1340 cm^{-1} band appears to correspond to an E_2-type mode of the main chain (O═C)—C^{α}—H moiety.

It is interesting to note that the fd difference band is close in wavenumber value though not identical to the unperturbed mode ($\nu_0 = 1347$ cm^{-1}) determined from eqs 5−7. This is not unexpected, since the fd coat protein α-helix may differ slightly from the more idealized α-helical structure of a synthetic polypeptide.

3. Raman Band of the (O═C)—C^{α}—H Group As an Indicator of α-Helix Orientation

(a) Rationale. Previous applications of polarized Raman spectroscopy to determine orientations of specific groups in macromolecular structures have required multiple spectral measurements employing different geometries for the incident electric vector with respect to the axis of orientation of the group being probed. For example, in determining the angle of inclination (θ) of the fd virion axis (c) with respect to the axis of the coat protein α-helix, Overman et al. (*10*) measured the following two polarized Raman intensities of the amide I band: I_{cc}, in which the incident and scattered electric vectors are along the direction of c, and I_{bb}, in which these vectors are along an axis (b) perpendicular to c. Although the relationship between the ratio of polarized Raman intensities (I_{cc}/I_{bb}) and θ is straightforward (*7*), accurate determination of I_{cc}/I_{bb} requires that in both I_{cc} and I_{bb} measurements the laser impinges on precisely the same cross-sectional area and depth of the sample. This is not always feasible experimentally, owing to the need to rotate the sample and electric vector with respect to one another without translocating the sample in the laser focal plane.

Because the 1340−1345 cm^{-1} Raman band—like amide I—arises from a vibration localized in the main chain of the α-helix, it also has the potential to serve as a marker of helix axis orientation, when properly investigated by polarized Raman spectroscopy of an oriented specimen. A single polarized Raman measurement of the (O═C)—C^{α}—H marker could suffice, if the intensity distribution ($A:E_2$) has been calibrated as a function of θ with the use of a standard of known helix inclination angle. Implementation of the (O═C)—C^{α}—H marker for this purpose offers the prospect that a reasonably accurate value of θ could be determined without the need for precise rotation of the sample with respect to the electric vector of the incident radiation. To further evaluate this prospect, we have investigated quantitatively the polarization of Raman scattering of oriented αPBLG in the 1340−1345 cm^{-1} interval. [In principle, a similar approach could be followed for oriented fd. In practice, however, overlap of the fd 1345 cm^{-1} band with the strongly polarized 1340 cm^{-1} band of the Trp-26 side chain severely complicates the spectral interpretation (*12*, *20*). In this regard, it should be noted that the A (1328 cm^{-1}) and E_2 (1341 cm^{-1}) components of the (O═C)—C^{α}—H marker of αPBLG are sufficiently well separated in the spectrum to permit analysis of the intensities without the complication of band overlap.]

(b) Calibration of the Polarization of the 1340−1345 cm^{-1} Raman band intensity in αPBLG. We have measured Raman band intensities in the 1250−1400 cm^{-1} region of the polarized Raman spectrum of αPBLG as a function of the angle of inclination (θ) of an oriented fiber with respect to the direction of the electric vector of the exciting radiation. The results are shown in Figure 6. Assuming that the helices of αPBLG are oriented perfectly along the fiber axis direction (*25*), these data provide an effective calibration curve for the Raman (O═C)—C^{α}—H markers (A and E_2 components at 1328 and 1341 cm^{-1}, respectively) as a function of θ. The results should be transferable to any other axially-symmetric fiber or crystal. For example, the polarized Raman spectrum observed for another α-helical macromolecule or assembly of unknown θ could be fitted to the data of Figure 6 to deduce the probable value of the helix inclination angle.

4. Application to Pf1 Virus: Inclination of the Coat Protein Helix Axis with Respect to the Virion Axis

The Pf1 virion, like fd, comprises several thousand copies of a small helical coat subunit (46 residues), which form a

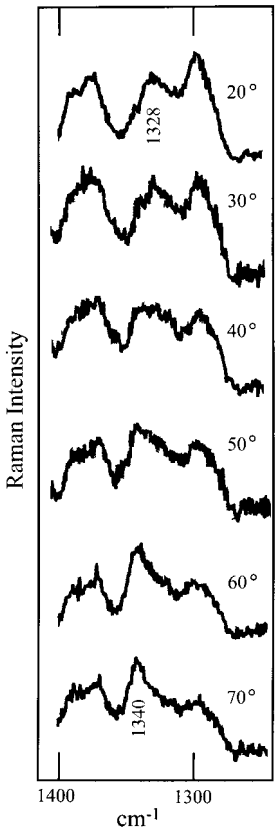

FIGURE 6: Polarized Raman spectra (514.5 nm) of an oriented αPBLG fiber obtained in the back-scattering geometry, with incident radiation propagated along the laboratory $+Z$ axis and scattered radiation collected along $-Z$. The electric vector of the exciting radiation was polarized in the direction of the laboratory *Y* axis, and the axis of the fiber was fixed in the *XY* plane, such that data could be collected when the fiber axis was rotated in increments of 10° through an angle between 20° and 70° with the *Y* axis, as labeled.

cylindrical sheath encapsidating a single-stranded DNA loop (*38*, *39*). Fiber X-ray diffraction shows that the coat subunit can be approximated as a single gently curved α-helix inclined at a small angle (θ) from the virion (*c*) axis (*40*). Here, we consider Pf1 as an assembly of α-helices oriented uniformly with respect to *c*, and use the data of Figure 6 to estimate θ. For this purpose, we examine the polarized Raman scattering of Pf1 in the 1250−1400 cm^{-1} region (Figure 7). The 45 peptide groups of the Pf1 coat subunit are the major contributors to the spectral region of interest, generating strong bands at 1340−1345 cm^{-1} from the (O═C)−C^{α}−H marker band and at 1300 cm^{-1} from the amide III mode of the α-helix. The very small contributions expected in this region of the spectrum from various aliphatic and polar side chains of the coat subunit, including four Leu (1321 cm^{-1}), six Ile (1321 cm^{-1}), five Val (1322 and 1364 cm^{-1}), one Lys (1323 and 1344 cm^{-1}), and two Ser (1342 cm^{-1}) residues (*21*), have been neglected. It is noteworthy that the Pf1 subunit contains no Trp side chain, which would otherwise interfere substantially in this spectral region (*12*, *28*, *29*).

Figure 7 shows that the I_{cc} spectrum of Pf1 is dominated by intense peaks at ∼1300 and ∼1322 cm^{-1}, whereas only a very weak shoulder occurs at ∼1343 cm^{-1}. Conversely, the I_{bb} spectrum is dominated by an intense band at 1343 cm^{-1}, with weak shoulders at ∼1322 and ∼1300 cm^{-1}. A

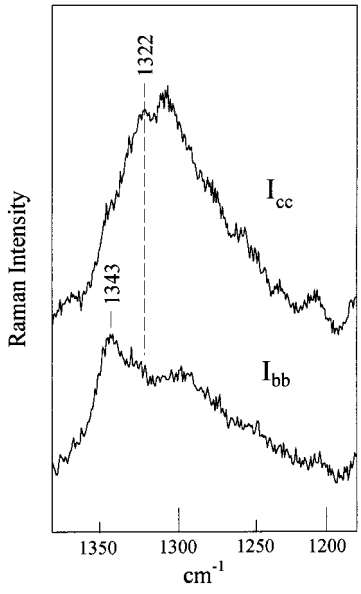

FIGURE 7: Polarized Raman spectra (1375−1200 cm^{-1}, excited at 514.5 nm) of Pf1 virus in *cc* (upper trace) and *bb* (lower trace) orientations. An aqueous droplet of the virus (∼50 mg/mL) was slowly drawn into an oriented fiber of about 0.5 mm thickness between glass rods of a fiber-pulling device maintained in a hygrostatic environment (92% relative humidity). Unidirectional orientation of virions within the fiber was assessed by observing that the maximum Raman intensity ratio was detected for parallel and perpendicular alignments of the fiber with respect to the electric vector of either the incident or scattered radiation.

very weak and poorly resolved feature is also observed near 1280 cm^{-1} in both the I_{cc} and I_{bb} spectra. One interpretation of these findings, consistent with previous unpolarized Raman studies of Pf1 and the foregoing analysis of the 1340−1345 cm^{-1} band in polarized spectra of fd and α-helical polypeptides, is the following: The α-helical coat subunit gives rise to a complex amide III band pattern, with components detectable at 1300 and 1280 cm^{-1} (*19*, *26*). The strong I_{cc}-polarized band at 1322 cm^{-1} is the Pf1 counterpart to the αPBLG A-species mode noted above (1328 cm^{-1}), and the strong I_{bb}-polarized band at 1343 cm^{-1} is the Pf1 counterpart to the αPBLG E_2-species mode (1341 cm^{-1}). Accordingly, the main chain (O═C)−C^{α}−H vibration of the α-helical subunit of Pf1 is presumed to generate two band components analogous to the A and E_2 modes observed in αPBLG. Although the strict helical symmetry (i.e., identical side chains) required for A- and E_2-species Raman-active modes does not apply rigorously to the Pf1 subunit, we propose that the approximate (main chain) symmetry is sufficient to account for the observed splitting of the (O═C)−C^{α}−H mode into components at 1343 and 1322 cm^{-1}.

An alternative—but in our view less likely—explanation for the data of Figure 7 is that two distinct vibrations of the Pf1 subunit occur in the 1320−1345 cm^{-1} interval, for which the polarizability oscillations are, respectively, close to perpendicular (1343 cm^{-1}) and parallel (1322 cm^{-1}) to the virion axis. No precedent for two such modes is evident from Raman spectra of other α-helical proteins and polypeptides. Intrahelical vibrational coupling between neighboring (O═C)−C^{α}−H groups, as discussed above, is therefore presumed to account for the observed band splitting.

Analysis of the (O═C)−C^{α}−H marker bands shows that in the *cc* spectrum of Pf1 (Figure 7, upper trace) the ratio of

intensities of the bands at 1322 and 1343 cm^{-1} ($I_{cc}^{1322}/I_{cc}^{1343}$) is best simulated by the A-species mode of αPBLG when the helix axis is tilted ∼20° from the vertical axis (Figure 6, top trace). Furthermore, the intensity ratio $I_{bb}^{1322}/I_{bb}^{1343}$ of the *bb* spectrum of Pf1 (Figure 7, lower trace) is best represented by the E_2-species mode of αPBLG when the helix axis is tilted ∼20° from the horizontal axis (i.e., ∼70° from the vertical axis) (Figure 6, bottom trace). Therefore, both the *cc* and *bb* polarizations are consistent with the conclusion that the coat protein α-helix in the native Pf1 assembly is tilted on average approximately 20° from the virion axis. The uncertainty in this result is estimated as ±10°.

CONCLUSIONS

The α-helical coat protein subunit of the filamentous virus fd exhibits a prominent band near 1340−1345 cm^{-1} which is diminished in intensity by $C^{\alpha}H$ deuteration and carbonyl ^{13}C isotope substitutions (*20*, *21*). These findings are consistent with assignment to a normal mode involving the C^{α}—H bend and C—C^{α} stretch internal coordinates of the main chain (O═C)—C^{α}—H moiety, but not involving the classic amide III peptide vibration. A corresponding band is evident in Raman spectra of α-helical poly-L-alanine (αPLA) and α-helical poly-γ-benzyl-L-glutamate (αPBLG). In these synthetic polypeptide α-helices, polarized Raman spectra suggest a main chain (O═C)—C^{α}—H mode of E_2 symmetry species near 1343 cm^{-1} and a counterpart of A symmetry near 1328 cm^{-1}.

Polarized Raman spectra of the filamentous virus Pf1 also demonstrate a pair of bands at 1322 and 1343 cm^{-1} assignable to the (O═C)—C^{α}—H moiety, the former intense in the I_{cc} spectrum (analogous to an A-type mode) and the latter intense in the I_{bb} spectrum (analogous to an E_2-type mode). Despite the fact that strict helical symmetry is not present in viral coat subunits, intrahelical coupling of peptides could account for the Raman band splitting observed in Pf1. The polarization anisotropy shows that the band components may be exploited as a novel probe of protein α-helix orientation. Application of this approach to the Pf1 subunit indicates a small average angle of inclination (20 ± 10°) of the α-helical coat protein axis with respect to the virion axis.

Previous polarized Raman studies of oriented fd virus have demonstrated that the helix axis of the coat subunit is also tilted at a small angle (16 ± 4°) from the virion axis (*10*). Thus, despite the different assembly architectures of fd (class I) and Pf1 (class II) virions, their respective α-helical coat subunits are tilted similarly in relation to the filament axis.

Recent investigations of Raman optical activity (ROA) of aqueous proteins reveal a prominent ROA band at approximately 1340−1345 cm^{-1}, which has been assigned to domains containing α-helical secondary structure (*17*, *41*, *42*). In the case of filamentous viruses, including fd, this ROA amplitude (measured as $I^R - I^L$, where I^R and I^L are the Raman scattered intensities of right- and left-circularly-polarized incident light) is observed at 1342 cm^{-1} and has been assigned to regions of the coat protein α-helical subunits that are highly hydrated (*42*). The observed ROA is consistent with the fact that right- and left-circularly-polarized light propagating along the α-helix axis should interact differently with the array of local (*ab*) tensor components. Interestingly, the 1342 cm^{-1} ROA feature also exhibits a large N-deuteration effect. This suggests a vibrational origin that includes the N−H bending internal coordinate. In future work, it will be of interest to investigate the effect of peptide (NH) deuteration on the A and E_2 modes examined here.

REFERENCES

1. Krimm, S., and Bandekar, J. (1986) *Adv. Protein Chem. 38*, 181−365.
2. Tsuboi, M. (1969) *Appl. Spectrosc. Rev. 3*, 45−90.
3. Miura, T., and Thomas, G. J., Jr. (1995) *Subcell. Biochem. 24*, 55−99.
4. Thomas, G. J., Jr. (1999) *Annu. Rev. Biophys. Biomol. Struct. 28*, 1−27.
5. Tsuboi, M., Ikeda, T., and Shindo, H. (1987) *Chem. Pharm. Bull. 35*, 4405−4409.
6. Norden, B., Kubista, M., and Kurucsev, T. (1992) *Q. Rev. Biophys. 25*, 51−170.
7. Tsuboi, M., and Thomas, G. J., Jr. (1997) *Appl. Spectrosc. Revs. 32*, 263−299.
8. Earnest, T. N., Herzfeld, J., and Rothschild, K. J. (1990) *Biophys. J. 58*, 1539−1546.
9. Hunt, J. F., Earnest, T. N., Bousche, O., Kalghatgi, K., Reilly, K., Horvath, C., Rothschild, K. J., and Engelman, D. M. (1997) *Biochemistry 36*, 15156−15176.
10. Overman, S. A., Tsuboi, M., and Thomas, G. J., Jr. (1996) *J. Mol. Biol. 259*, 331−336.
11. Takeuchi, H., Matsuno, M., Overman, S. A., and Thomas, G. J., Jr. (1996) *J. Am. Chem. Soc. 118*, 3498−3507.
12. Tsuboi, M., Overman, S. A., and Thomas, G. J., Jr. (1996) *Biochemistry 35*, 10403−10410.
13. Diem, M., Lee, O., and Roberts, G. M. (1992) *J. Phys. Chem. 96*, 548−554.
14. Jordan, T., and Spiro, T. G. (1994) *J. Raman Spectrosc. 25*, 537−543.
15. Chi, Z., and Asher, S. A. (1998) *Biochemistry 37*, 2865−2872.
16. Overman, S. A., and Thomas, G. J., Jr. (1998) *J. Raman Spectrosc. 29*, 23−29.
17. Teraoka, J., Bell, A. F., Hecht, L., and Barron, L. D. (1998) *J. Raman Spectrosc. 29*, 67−71.
18. Lee, S.-H., and Krimm, S. (1998) *J. Raman Spectrosc. 29*, 73−80.
19. Thomas, G. J., Jr., Prescott, B., and Day, L. A. (1983) *J. Mol. Biol. 165*, 321−356.
20. Overman, S. A., and Thomas, G. J., Jr. (1998) *Biochemistry 37*, 5654−5665.
21. Overman, S. A., and Thomas, G. J., Jr. (1999) *Biochemistry 38*, 4018−4027.
22. Fanconi, B., Tomlinson, B., Nafie, L. A., Small, W., and Peticolas, W. L. (1969) *J. Chem. Phys. 51*, 3993−4005.
23. Lee, S.-H., and Krimm, S. (1998) *Biopolymers 46*, 283−317.
24. Tsuboi, M. (1962) *J. Polym. Science 59*, 139−153.
25. Wilser, W. T., and Fitchen, D. B. (1975) *J. Chem. Phys. 62*, 720−724.
26. Thomas, G. J., Jr., and Murphy, P. (1975) *Science 188*, 1205−1207.
27. Berkowitz, S. A., and Day, L. A. (1976) *J. Mol. Biol. 102*, 531−547.
28. Aubrey, K. L., and Thomas, G. J., Jr. (1991) *Biophys. J. 60*, 1337−1349.
29. Overman, S. A., and Thomas, G. J., Jr. (1995) *Biochemistry 34*, 5440−5451.
30. Miyazawa, T., Shimanouchi, T., and Mizushima, S.-I. (1958) *J. Chem. Phys. 29*, 611−616.
31. Torii, H., Tatsumi, T., and Tasumi, M. (1998) *J. Raman Spectrosc. 29*, 537−546.
32. Lin-Vien, D., Colthup, N. B., Fateley, W. G., and Grasselli, J. G. (1991) *The Handbook of Infrared and Raman Characteristic Frequencies of Organic Molecules*, Academic Press, Inc., San Diego, CA.
33. Fukushima, K., Onishi, T., Shimanouchi, T., and Mizushima, S. (1959) *Spectrochim. Acta 13*, 236−241.

34. Diem, M., Polavarapu, P. L., Oboodi, M. R., and Nafie, L. A. (1982) *J. Am. Chem. Soc. 104*, 3329−3336.
35. Nakagawa, I., and Mizushima, S. (1955) *Bull. Chem. Soc. Jpn. 28*, 589−594.
36. Higgs, P. W. (1953) *Proc. R. Soc. London A220*, 472−485.
37. Miyazawa, T. (1960) *J. Chem. Phys. 32*, 1647−1652.
38. Liu, D. J., and Day, L. A. (1994) *Science 256*, 671−674.
39. Hill, D. F., Short, N. J., Perham, R. N., and Peterson, G. B. (1991) *J. Mol. Biol. 218*, 351−364.
40. Gonzalez, A., Nave, C., and Marvin, D. A. (1995) *Acta Crystallogr. D51*, 792−804.
41. Wilson, G., Ford, S. J., Cooper, A., Hecht, L., Wen, Z. Q., and Barron, L. D. (1995) *J. Mol. Biol. 254*, 747−760.
42. Blanch, E. W., Bell, A. F., Hecht, L., Day, L. A., and Barron, L. D. (1999) *J. Mol. Biol. 290*, 1−7.

BI9918846